

FINAL REPORT (SNN 114490)

Project title: The role of lymph vessels in malignant pleural mesothelioma

Home Institute: National Koranyi Institute of Pulmonology, Budapest, Hungary

Rationale and Aim

This project aimed to clarify the biological and clinical significance of the lymph vasculature in the progression of MPM (malignant pleural mesothelioma), a devastating thoracic malignancy with dismal prognosis largely due to resistance to current therapeutic modalities

Results

In vitro results

As proposed in our original research plan, we further analyzed the gene expression profiles of our MPM cell lines and validated the mRNA expressions of the different (lymph)angiogenic molecules (Fig.1) and their receptors (Fig.2).

Next, we measured the protein levels of different (lymph)angiogenic molecules (VEGF-A, VEGF-C, apelin, endothelin-1, FGF2, FGF18) in normal mesothelial cells (NP1, NP2) and in 18 different human MPM cell lines by ELISA. Of note, we found significantly elevated VEGF-A, VEGF-C and decreased endothelin-1 levels in MPM cells (vs. NP1 and NP2 cell lines).

We also established an in vitro vascular/lymphatic model system which allows the quantitative analysis of how diffusive growth factors (like VEGF isoforms) effect lymphatic and blood capillary vascular sprout formation. The assay utilizes aggregates made of lymphatic endothelial cells, placed in a 3D fibrin gel environment. Co-cultures of endothelial and tumor spheroids reveal how MPM cell lines can modulate endothelial sprouting by diffusive factors. Spheroids of distinct MPM cell lines inhibit endothelial sprout growth to various degrees. By quantitative morphometric analysis we established that M38K spheroids are most repulsive, while p31 spheroids are the most permissive -- with SPC111 spheroids in between these two extremes (Fig.3.)

In vivo results

By using confocal (whole mount samples and frozen sections of the diaphragm) and electron microscopy, we also investigated the vascularisation and growth of orthotopically implanted human P31 and SPC111 MPM cells. Furthermore, we assessed the motility and invasion of P31 and SPC111 cells and spheroids in vitro. In this set of mouse experiments, both MPM lines induced the early development of submesothelial microvascular plexuses bulging into the pleural space and covering large areas of the diaphragm including regions distant from tumor colonies. The development of these microvascular networks occurred due to both intussusceptive angiogenesis and endothelial sprouting and was faster when VEGF-A-overexpressing MPM cells were implanted. Importantly, SPC111 cells showed different behaviour to P31 cells. P31 colonies invaded and thus incorporated the tumor-induced capillary plexuses from the earliest stages of MPM nodule formation (4-5 days post inoculation) (Fig.4.A). In contrast, SPC111 colonies pushed the capillary plexuses away and thus remained avascular for up to three weeks (Fig.4.B). In support of this, P31 cells and spheroids exhibited significantly higher 2D motility (spreading) on plastic and 3D invasion in collagen and collagen/fibronectin gels. The key event in in vivo SPC111 vascularization was a desmoplastic response beneath the tumor nodules. This desmoplastic matrix was continuously engulfed by the SPC111 nodules resulting in the appearance of intratumoral collagen-containing desmoplastic tissue trunks providing a

route for endothelial sprouting from the diaphragm. Based on these in vivo studies, we concluded that there are two distinct growth and vascularization patterns of orthotopically implanted human MPM tumors in mice. In the invasive growth pattern, MPM cells invade and thus co-opt the peritumoral capillary plexuses of the pleura. In the pushing/desmoplastic growth pattern, MPM cells fail to invade the peritumoral capillary plexuses. Instead, they induce a desmoplastic response within the underlying pleura which allows endothelial sprouting and the development of a nutritive vasculature. The publication of these latter in vivo findings is in preparation.

Human studies

In another set of experiments, we found that plasma VEGF-C (the key lymphangiogenic factor) protein levels are significantly elevated in MPM patients (n=63) as compared to healthy controls (n=14) and patients with non-malignant pleural diseases (n=13, p=0.031, Figure 5.A). VEGF-C levels also correlated with more advanced disease stage (p=0.039, Fig. 5.B.). Importantly, high plasma VEGF-C level was also associated with poor overall survival (p<0.01, Fig. 5.C.). The publication of these human findings is also in preparation.

In part with the support of the current proposal we also could demonstrate that PB levels of the anti-lymphangiogenic factor activin-A (ActA) are also elevated in MPM patients. In this study, which was published in the EJC (Eur J Cancer 2016; 63:64-73.) plasma samples were collected from 129MPM patients in four institutions at the time of diagnosis or before surgical resection. Samples from 45 healthy individuals and from 16 patients with non-malignant pleural diseases served as controls. Circulating activin A was measured by ELISA and correlated to clinicopathological variables. We reported that circulating activin A measurement may support the histological classification of MPM and at the same time help to identify epithelioid MPM patients with poor prognosis. For details, please see: <https://www.ncbi.nlm.nih.gov/pubmed/27288871>

Additional important studies that have been published with the partial support of the current grant were the demonstration that the multi-target small molecule anticancer drug nintedanib shows promising effectiveness in stopping the growth and vascularization of human MPM in preclinical models (Laszlo et al. Clin Cancer Res 2018; 24:3729-3740.) and, furthermore, that focal adhesion kinase (FAK) inhibition can interfere with MPM spheroid growth in vitro and tumor growth and angiogenesis in vivo (J Mol Med 2019; 97:231-242). For details, please see <https://www.ncbi.nlm.nih.gov/pubmed/29724868> and <https://www.ncbi.nlm.nih.gov/pubmed/30539198>, respectively.

Figures

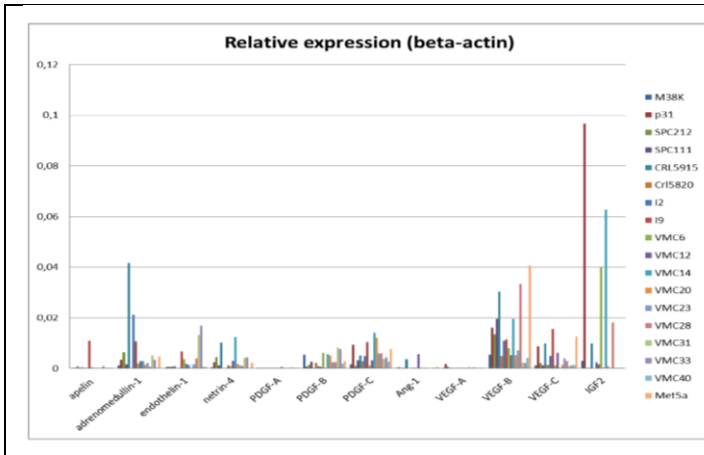


Fig.1. mRNA expression of different (lymph)angiogenic factors (apelin, adrenomedullin-1, endothelin-1, netrin-4, PDGF-A, PDGF-B, PDGF-C, Ang-1, VEGF-A, VEGF-B, VEGF-C, IGF2) was measured in eight international MPM cell lines (M38K, p31, SPC212, SPC111, CRL5915, CRL5820, I2, I9), in eight MPM cell lines established by our group (VMC12, VMC14, VMC20, VMC23, VMC28, VMC31, VMC33, VMC40) and in the immortalized non-malignant mesothelial cell line Met5A. Reference gene: β -actin

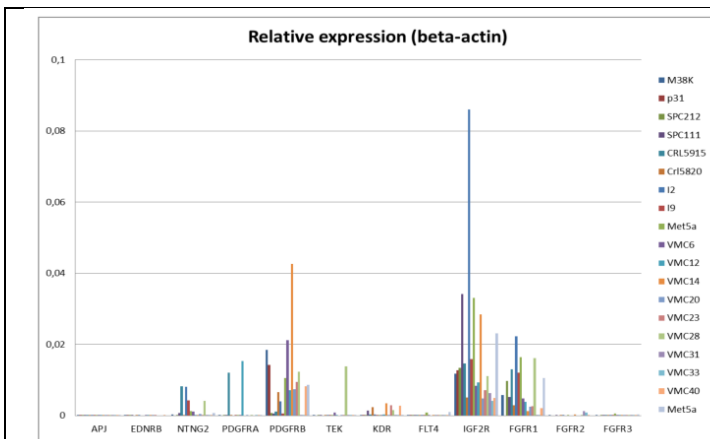


Fig.2. mRNA expression of different (lymph)angiogenic factor receptors (APJ, apelin receptor; EDNRB, endothelin receptor; PDGFR-A,B; TEK, Ang-1 receptor, KDR, VEGF receptor-2; FLT4, VEGF receptor 3; IGF2R, Insulin-like growth factor 2 receptor; FGFR2, fibroblast growth factor receptor-2; FGFR3, fibroblast growth factor receptor-3) was measured in eight international MPM cell lines (M38K, p31, SPC212, SPC111, CRL5915, CRL5820, I2, I9), in eight MPM cell lines established by our group (VMC12, VMC14, VMC20, VMC23, VMC28, VMC31, VMC33, VMC40) and in the immortalized non-malignant mesothelial cell line Met5A. Reference gene: β -actin

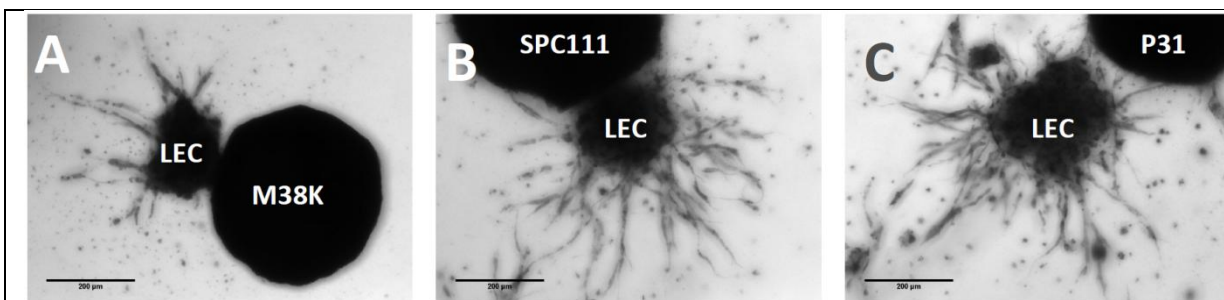


Fig.3. Spheroids of MPM lines can repel, to various extents, endothelial sprouts. Semaphorins are known regulators of endothelial guidance, and were reported to be produced by MPM cells. Our qPCR analysis revealed that M38K and SPC111 cells produce 10-fold more sema3f and sema3e isoforms, respectively, than p31 cells do. Both sema3f and sema3e are well documented chemorepellents of endothelial cell migration. Thus, several MPM lines can affect the spatial orientation of growing vascular sprouts and vessels. Spheroids of three MPM cell lines chosen on the basis of semaphorin expression profiles were co-cultured with aggregates of lymphatic endothelial cells (LEC) in fibrin gel for 4 days. A: High semaphorin-3b expression of M38K cells repel sprouts and give rise to a highly anisotropic endothelial sprout morphology. B: A lower expression level of SPC111 cells creates a less repellent environment for sprout growth. C: Sprouts approach but do not grow into P31 spheroids, which have the lowest semaphorin-3b expression.

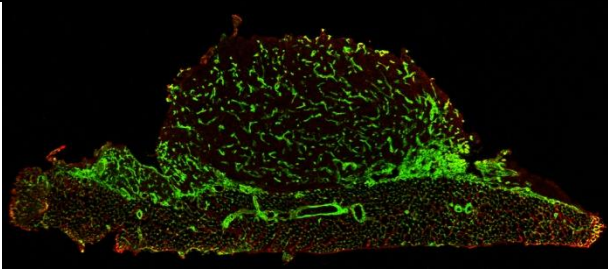


Fig.4.A. P31 colony on the diaphragm 42 days following inoculation. Note the dense intratumoral vasculature. On both sides of the colony microvascular plexuses are present. CD31 (*green*), laminin (*red*)

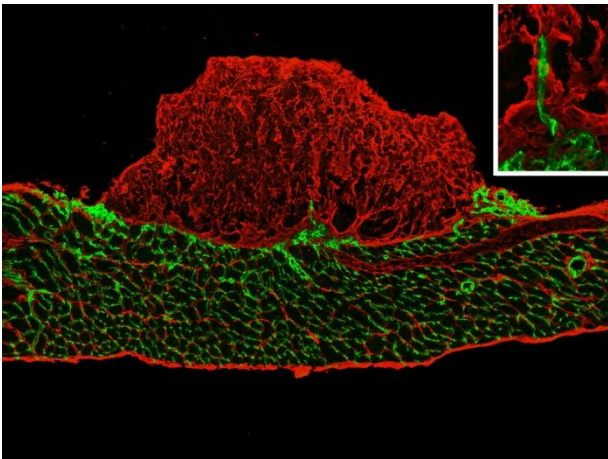


Fig4.B. SPC111 colony 28 days following inoculation. Endothelial sprout, located inside a fibronectin-containing extracellular matrix bundle, projects towards the tumor center. Inset shows the sprout at higher power. CD31 (*green*), fibronectin (*red*)

